Selective IRAK4 Inhibition Attenuates Disease in Murine Lupus Models and Demonstrates Steroid Sparing Activity

Shailesh Dudhgaonkar,* Sourabh Ranade,* Jignesh Nagar,* Siva Subramani,* Durga Shiv Prasad,* Preethi Karunanithi,* Ratika Srivastava,* Kamala Venkatesh,* Sabariya Selvam,* Prasad Krishnamurthy,* T. Thanga Mariappan,* Ajay Saxena,* Li Fan,† Dawn K. Stetsko,† Deborah A. Holloway,† Xin Li,‡ Jun Zhu,§ Wen-Pin Yang,§ Stefan Ruepp,¶ Satheesh Nair,* Joseph Santella,‖ John Duncia,‖ John Hynes,‖ Kim W. McIntyre,† and Julie A. Carman†

The serine/threonine kinase IL-1R–associated kinase (IRAK)4 is a critical regulator of innate immunity. We have identified BMS-986126, a potent, highly selective inhibitor of IRAK4 kinase activity that demonstrates equipotent activity against multiple MyD88-dependent responses both in vitro and in vivo. BMS-986126 failed to inhibit assays downstream of MyD88-independent receptors, including the TNF receptor and TLR3. Very little activity was seen downstream of TLR4, which can also activate an MyD88-independent pathway. In mice, the compound inhibited cytokine production induced by injection of several different TLR agonists, including those for TLR2, TLR7, and TLR9. The compound also significantly suppressed skin inflammation induced by topical administration of the TLR7 agonist imiquimod. BMS-986126 demonstrated robust activity in the MRL/*lpr* and NZB/NZW models of lupus, inhibiting multiple pathogenic responses. In the MRL/*lpr* model, robust activity was observed with the combination of suboptimal doses of BMS-986126 and prednisolone, suggesting the potential for steroid sparing activity. BMS-986126 also demonstrated synergy with prednisolone in assays of TLR7- and TLR9-induced IFN target gene expression using human PBMCs. Lastly, BMS-986126 inhibited TLR7- and TLR9-dependent responses using cells derived from lupus patients, suggesting that inhibition of IRAK4 has the potential for therapeutic benefit in treating lupus. ***The Journal of Immunology*****, 2017, 198: 1308–1319.**

Interleukin-1R–associated kinase (IRAK)4 is a serine/threonine kinase required for signal transduction downstream of the IL-1 receptor family and is a subset of TLRs. The TLR family recognizes molecular patterns derived from infectious organisms, including bacteria, fungi, parasites, and viruses (1). Ligand binding to the receptor induces dimerization and recruitment of adaptor molecules to a conserved cytoplasmic motif in the receptor termed the Toll/IL-1R (TIR) domain. With the exception of TLR3, all TLRs recruit the adaptor MyD88. The IL-1 receptor family also contains a cytoplasmic TIR motif and recruits MyD88 upon ligand binding (2). Members of the IRAK family of serine/threonine kinases are recruited to the receptor via interactions with MyD88. The family consists of four members, IRAK1, IRAK2, IRAK3 (also known as IRAK-M), and IRAK4. Several lines of evidence indicate that IRAK4 plays a critical and nonredundant role in initiating signaling via MyD88-dependent TLRs and IL-1R family members. Structural data confirm that IRAK4 directly interacts with MyD88 and subsequently recruits either IRAK1 or IRAK2 to the receptor complex to facilitate downstream signaling (3). IRAK4 directly phosphorylates IRAK1 to induce downstream signaling to the E3 ubiquitin ligase TNFR-associated factor 6, resulting in activation of the serine/threonine kinase TAK1 with subsequent activation of the NF-κB pathway and MAPK cascade (4). A subset of human patients was identified who lack IRAK4 expression (5). Cells from these patients fail to respond to all TLR agonists, with the exception of TLR3, as well as to members of the IL-1 family, including IL-1β and IL-18 (6). Deletion of IRAK4 in mice results in a severe block in IL-1, IL-18, and all TLR-dependent responses with the exception of TLR3 (7). In contrast, deletion of either IRAK1 (8, 9) or IRAK2 (10) results in partial loss of signaling. Furthermore, IRAK4 is the only member of the IRAK family whose kinase activity has been shown to be required for the initiation of signaling. Replacement of wild-type IRAK4 in the mouse genome with a kinase-inactive mutant (KDKI) impairs signaling via all MyD88-dependent receptors, including IL-1, IL-18, and all TLRs with the exception of TLR3 (11–13).

*Biocon Bristol-Myers Squibb Research Center, Bangalore 560099, India; †Immunology Discovery, Bristol-Myers Squibb, Princeton, NJ 08543; ‡Lead Evaluation, Bristol-Myers Squibb, Princeton, NJ 08543; §Translational Technologies, Bristol-Myers Squibb, Hopewell, NJ 08525; ¶Discovery Toxicology, Bristol-Myers Squibb, Princeton, NJ 08543; and ‖Discovery Chemistry, Bristol-Myers Squibb, Princeton, NJ 08543

ORCIDs: 0000-0003-4242-8542 (S. Ranade.); 0000-0003-3883-6447 (J.N.); 0000-0003-1746-5886 (P. Karunanithi); 0000-0001-6308-553X (R.S.); 0000-0002-8209-130X (P. Krishnamurthy); 0000-0002-7582-849X (D.K.S.); 0000-0002-9176-6786 (J.Z.).

Received for publication April 1, 2016. Accepted for publication November 22, 2016.

The data presented in this article have been submitted to the National Center for Biotechnology Information Gene Expression Omnibus (http://www.ncbi.nlm.nih.gov/geo/) under accession number GSE81527.

Address correspondence and reprint requests to Dr. Julie A. Carman, Bristol-Myers Squibb, P.O. Box 4000, Mail Stop K24-03, Princeton, NJ 08543. E-mail address: julie.carman@bms.com

The online version of this article contains supplemental material.

Abbreviations used in this article: DC, dendritic cell; dsDNA, double-stranded DNA; HTRF, homogeneous time-resolved fluorescence; IRAK, IL-1R–associated kinase; LTA, lipoteichoic acid; NGAL, neutrophil gelatinase-associated lipocalin; ODN, oligodeoxynucleotide; pDC, plasmacytoid dendritic cell; PEG, polyethylene glycol; qPCR, quantitative PCR; RNP, ribonucleoprotein; TIR, Toll/IL-1R; TRIF, Toll/IL-1R domain–containing adaptor-inducing IFN-β.

Dysregulated TLR signaling has been implicated in several autoimmune and inflammatory diseases. TLR7 and TLR9 have been implicated in the pathophysiology of lupus (14). Some of the key characteristics of lupus include high levels of autoantibodies specific for nucleic acid and nucleic acid–binding proteins, as well as high expression of IFN-regulated genes by peripheral blood leukocytes (15). Immune complexes of autoantibodies bound to nucleic acids are taken up by Fcγ receptors that mediate delivery of the nucleic acids to endosomes where they stimulate TLR7 and TLR9 (16). Activation of these TLRs in plasmacytoid dendritic cells (pDCs) drives production of high levels of type I IFNs (17). Stimulation of TLR7 and TLR9 in B cells has been shown to potentiate their differentiation of plasma cells, thereby contributing to autoantibody production (18). Therefore, inhibition of IRAK4 has the potential to block multiple pathogenic responses. In this study we describe the identification of a potent, highly selective inhibitor of IRAK4 that demonstrated activity against multiple MyD88-dependent responses both in vitro and in vivo. We observed robust efficacy in two different mouse models of lupus, the MRL/*lpr* and NZB/NZW models. In the MRL/*lpr* model the compound enhanced the efficacy of a suboptimal dose of prednisolone, suggesting the potential for steroid sparing activity. These data suggest that inhibition of IRAK4 is a promising approach for the treatment of lupus.

Materials and Methods

Kinase assays

For IRAK4 enzyme assays, 1.5 μM peptide substrate (FITC-AHA-IPTSPITTTYFFFKKK-OH) and 500 μM ATP were used in an assay buffer containing 20 mM HEPES, 10 mM $MgCl_2$, 0.015% Briji-35, and 4 mM DTT. Human recombinant IRAK4 was used at 2 nM in the assays. The kinase reactions were initiated by combining the kinase, fluoresceinated peptide substrate, ATP, and test compound in assay buffer. The reaction was incubated at room temperature and terminated with the addition of 45 μl of 35 mM EDTA to each sample. The reaction mixture was analyzed on the Caliper LabChip 3000 (Caliper, Hopkinton, MA) by electrophoretic separation of the fluorescent substrate and phosphorylated product. Inhibition data were calculated by comparison with no enzyme control reactions for 100% inhibition and vehicle-only reactions for 0% inhibition. Dose response curves were generated to determine the IC_{50} of kinase activity by nonlinear regression analysis. The other 214 kinase assays in the panel were either run in this format or using a homogeneous time-resolved fluorescence (HTRF) platform. HTRF assays were conducted in 1536-well plates with 2 μl of reactions prepared from addition of enzyme tagged either with GST or histidine (1 nM), tag-specific Ab (0.2 nM), a labeled small molecule probe, and test compounds in assay buffer (20 mM HEPES [pH 7.4], 10 mM $MgCl_2$, 0.015% Brij35, 4 mM DTT, and 0.05 mg/ml BSA). Following a 1-h incubation at room temperature, the HTRF signal was measured on an EnVision plate reader (excitation, 340 nm; emission, 520/495 nm).

BMS-986126 was also tested against a panel of 338 kinase assays using ^{33}P incorporation at Reaction Biology (Malvern, PA). Each kinase was tested individually in duplicate with 1 μM BMS-986126 and 10 μM ATP.

Human PBMC assays

PBMCs from human donors were purified from whole blood, resuspended in media containing 10% FBS and different concentrations of BMS-986126, and incubated for 30 min at 37°C. Different TLR agonists, IL-1β, or TNF-α was added, and incubations were continued for 5 h at 37°C. For TLR3 and IL-18 plus IL-12–induced responses, cultures continued for 24 h. The TLR agonists used include lipoteichoic acid (LTA; InvivoGen, catalog no. tlrl-pslta, final concentration of 10 μg/ml), LPS (Sigma-Aldrich, catalog no. L2637, final concentration of 100 ng/ml), gardiquimod (InvivoGen, catalog no. tlrl-gdq, final concentration of 5 μg/ml), flagellin (InvivoGen, catalog no. tlrl-slfa, final concentration of 10 ng/ml), and polyinosinic-polycytidylic acid [poly(I:C); InvivoGen, catalog no. tlrl-pic, final concentration of 40 μg/ml]. IL-1β (R&D Systems, no. 201-LB-025) and TNF-α (R&D Systems, no. 210-TA-010) were added at a concentration of 10 ng/ml. IL-18 (R&D Systems, no. B0001-5, 10 ng/ml) was combined with IL-12 (PeproTech, no. 200-12, 0.25 ng/ml) to stimulate some groups. At the end of the stimulation period, culture supernatants were harvested by centrifugation and analyzed for cytokine levels by ELISA. Cultures stimulated with LTA, LPS, flagellin, and gardiquimod were analyzed for IL-6 levels (BD Biosciences Singapore, catalog no. 555220). Cultures stimulated with poly(I:C) were analyzed for IP-10 levels (BD Biosciences, catalog no. 550926). Cultures stimulated with IL-1β and TNF-α were analyzed for IL-8 levels (BD Biosciences, no. 555244). Cultures stimulated with IL-18 plus IL-12 were analyzed for IFN-γ levels (BD Biosciences, no. 555142).

For TLR7- and TLR9-induced IFN-α production, PBMCs from human donors were purified from whole blood, resuspended in media containing 10% FBS, plated in a 96-well ELISPOT plate that was precoated with an Ab to human IFN-α (Mabtech, catalog no. 3425-2AW-PLUS) with different concentrations of BMS-986126. Cells were cultured with compound for 30 min at 37°C. Stimulus was added, either 5 μg/ml gardiquimod (InvivoGen, catalog no. TLRL-gdq) or 0.3 nM oligodeoxynucleotide (ODN)2216 (InvivoGen, catalog no. tlrl-2216), and cultures were continued for an additional 24 h for gardiquimod and an additional 6 h for ODN2216. Spots were developed according to kit instructions and counted on an ImmunoSpot reader (Cellular Technology, Shaker Heights, OH).

For signaling assays, PBMCs from human donors were purified from whole blood, resuspended in media containing 10% FBS, and cultured with different concentrations of BMS-986126 for 30 min at 37°C. Cells were stimulated for 15 min with either 10 μg/ml LTA (InvivoGen, catalog no. tlrl-pslta) or 100 ng/ml LPS (Sigma-Aldrich, no. L2637). Some groups were stimulated with 10 μg/ml gardiquimod (InvivoGen, catalog no. tlrl-gdq) for 30 min. At the end of the stimulation, cells were harvested by centrifugation and lysed in buffer containing phosphatase and protease inhibitors (Cell Signaling Technology, no. 9803). Lysates were analyzed in the Simple Western size-based capillary electrophoresis system (ProteinSimple Sally Sue; ProteinSimple, San Jose, CA). The size-separated proteins were probed with Abs specific for phospho-IKKα/β ($Ser^{176/180}$; Cell Signaling Technology, no. 2697), phospho-ERK (Thr^{202}/Tyr^{204}; Cell Signaling Technology, no. 9101), or actin (Sigma-Aldrich, no. A3854), visualized using labeled secondary Abs, and quantitated using the manufacturers' software. For each lane, the area of the phospho-IKKα/β or phospho-ERK band was normalized to the area of the actin band.

For TLR7- and TLR9-induced IFN response genes, PBMCs from human donors, both normal healthy volunteers and lupus patients, were purified from whole blood, resuspended in serum-free media, plated in a 96-well plate with different concentrations of BMS-986126 and cultured for 30 min at 37°C. In some experiments, cells were cultured with suboptimal concentrations of BMS-986126 and prednisolone alone and in combination. Cells were stimulated with either 0.5 μg/ml gardiquimod (InvivoGen, catalog no. tlrl-gdq), 300 nM ODN2216 (InvivoGen, catalog no. tlrl-2216), or 0.02 μl of UV-inactivated influenza virus (Advanced Biotechnologies, catalog no. 10-273-500) for an additional 5 h. In some experiments, cells were stimulated with ribonucleoprotein (RNP)-specific Abs complexed with necrotic cell lysate. RNA was isolated from cell pellets, reverse transcribed to cDNA, and used in quantitative PCR (qPCR) assays. Amplified genes included IFIT1, MX1, and the housekeeping gene GAPDH. Primers were as follows: IFIT1, forward, 5′-CTCCTTGGGTTCGTCTA-TAAATTG-3′ reverse, 5′-AGTCAGCAGCCAGTCTCAG-3′; MX1, forward, 5′-TACCAGGACTACGAGATTG-3′, reverse, 5′-TGCCAGGAAGGTCTAT-TAG-3′; and GAPDH, forward, 5′-AATTCCATGGCACCGTCAAG-3′, reverse, 5′-GAAGACGCCAGTGGACTCCA-3′

For global gene expression profiling, PBMCs from two independent donors were isolated, pretreated with 5 μM BMS-986126 or DMSO (vehicle) for 30 min at 37°C, and then stimulated for 5 h with 5 μg/ml gardiquimod. Total RNA was isolated from the cells with a Qiagen RNeasy mini kit (Qiagen, catalog no. 74104). Total RNA was then treated with DNase I and cleaned up with a Qiagen RNeasy MiniElute cleanup kit (Qiagen, catalog no. 74204). The RNA concentrations were determined by NanoDrop, and RNA quality was evaluated using Experion (Bio-Rad Laboratories). All target-labeling reagents were purchased from Affymetrix (West Sacramento, CA). Double-stranded cDNAs were synthesized from 1 μg of total RNA through reverse transcription with an oligo(dT) primer containing the T7 RNA polymerase promoter and double strand conversion using the cDNA synthesis system. Biotin-labeled cRNA was generated from the cDNA and used to probe the Human Genome U219 array, comprising 49,293 probe sets and representing >20,000 human genes, using the GeneTitan multi-channel instrument (Affymetrix). All cDNA and cRNA target preparation steps were processed on a Caliper GeneChip Array Station from Affymetrix. Array hybridization, washing, and scanning were performed according to the manufacturer's recommendations. The resulting files were processed using the robust multiarray analysis algorithm. Genes with a fold change ≥1.5 or smaller than or equal to −1.5 and with a p value of <0.005 in both donors are considered to be significantly changed. The heat maps of changed genes were generated by a hierarchical clustering tool from Partek Genomics Suite (Partek,

St. Louis, MO). The data have been deposited in the National Center for Biotechnology Information gene expression omnibus with the GEO accession no. GSE81527 (http://www.ncbi.nlm.nih.gov/geo/).

Mouse and human whole blood assays

Human whole blood was drawn into ACD-A anticoagulant and incubated with different concentrations of BMS-986126 in media for 30 min at 37˚C. Blood was stimulated with 10 μg/ml LTA (InvivoGen, no. tlrl-pslta) for an additional 5 h. IL-6 levels in the plasma were measured by ELISA (BD Biosciences, no. 555220). Mouse whole blood was assayed as described for human whole blood. Mouse IL-6 levels in the plasma were measured by ELISA (BD Biosciences, no. 555240).

In vivo mouse studies

All animal experiments were conducted according to the Committee for the Purpose of Control and Supervision of Experiments on Animals (registration no. 1089/RO/bc/2007/CPCSEA), Government of India guidelines. All experimental procedures were conducted under the protocols approved by the Institutional Animal Ethics Committee and performed in an American Association for the Accreditation of Laboratory Animal Care–accredited facility.

For LTA-induced IL-6, female BALB/c mice were randomized into five groups based on body weight and assigned as either vehicle (40% 20 mM citrate buffer, 45% polyethylene glycol [PEG]–300, 10% EtOH, 5% Pluronic F-68) or BMS-986126 at 0.1, 0.3, 1.0, and 3.0 mg/kg. Mice were challenged i.p. with 25 mg/kg body weight of LTA (Sigma-Aldrich, catalog no. L2515) 30 min after oral administration of either vehicle or compound. Ninety minutes after LTA injection, mice were bled and plasma IL-6 levels were estimated by ELISA (BD Biosciences, catalog no. 555240).

For TLR9-induced IFN-α, 12-wk-old male C57BL/6 mice were randomized into three groups based on body weight. Mice in these respective groups were dosed orally with either vehicle (40% 20 mM citrate buffer, 45% PEG-300, 10% EtOH, 5% Pluronic F-68) or BMS-986126 at 1.0 and 3.0 mg/kg. Mice were given 2.5 μg/mouse of CpG-ODN (InvivoGen, no. tlrl-1585-1) i.v. 30 min after dosing with either vehicle or compound. Mice were bled 2, 8, and 24 h after the CpG-ODN challenge, and plasma IFN-α levels were measured by ELISA (PBL Assay Science, Piscataway, NJ, catalog no. 42120-2).

For TLR7-induced cytokines, 12-wk-old male C57BL/6 mice were randomized into three groups based on body weight. Mice in these respective groups were dosed orally with either vehicle (40% 20 mM citrate buffer, 45% PEG-300, 10% EtOH, 5% Pluronic F-68) or BMS-986126 at 1.0 and 3.0 mg/kg. Mice were given 5 mg/kg gardiquimod (InvivoGen, no. tlrl-gdq-5) i.p. 30 min after compound dosing. Mice were bled 2, 8, and 24 h after challenge, and plasma IFN-α and IL-6 levels were measured by ELISA as above.

Imiquimod-induced skin inflammation

Skin inflammation was induced in male C57BL/6 mice by application of imiquimod cream (Aldara, 3M Pharmaceuticals) on the shaved back region of the mice every day for 6 d. C57BL/6 (six to eight mice per group) mice were randomly divided into five different treatment groups, respectively, and were treated once daily orally for 6 d with BMS-986126 at 0.3, 1.0, 3.0, and 10.0 mg/kg. Vehicle control mice received 40% 20 mM citrate buffer, 45% PEG-300, 10% EtOH, and 5% Pluronic F-68. Disease severity was monitored daily by recording skin thickness, erythema, and scaling. Skin thickness was measured using a micrometer. Erythema and scaling were scored using a scale of 0–4 (0, no erythema/scaling; 1, slight redness/scaling; 2, moderate redness/scaling; 3, marked redness/scaling; and 4, severe redness/scaling). One day before termination of the experiment, mice were bled at various time points to capture the complete pharmacokinetic profile of the test compound. At the end of experiment, all animals were euthanized by CO_2 asphyxiation, and skin samples were submitted for histology. Skin samples were fixed in 10% neutral buffered formalin, embedded in paraffin, and stained with H&E. Disease severity was evaluated microscopically for epidermal hyperkeratosis, parakeratosis, acanthosis, and microabscess and infiltration of inflammatory cells and follicular hyperplasia in dermis. The lesions were scored on the severity scale of 0–4 (0, unremarkable; 1, minimal; 2, mild; 3, moderate; and 4, marked).

*MRL/*lpr *SLE model*

Male MRL/*lpr* mice 12–14 wk of age (The Jackson Laboratory, Bar Harbor, ME) were screened and randomized based on the titers of anti-double–stranded DNA (dsDNA) Abs. Animals were treated orally, once daily for 8 wk with BMS-986126 at 0.3, 1, 3, and 10 mg/kg. Vehicle controls were dosed daily with 40% 20 mM citrate buffer, 45% PEG-300, 10% EtOH, and 5% Pluronic F-68. After 8 wk of dosing, all groups were evaluated for different disease-associated end points, including proteinuria, urine creatinine, urine neutrophil gelatinase-associated lipocalin (NGAL), dsDNA-specific autoantibody titers, blood urea nitrogen, plasma concentrations of IL-10 and IL-12p40, and percentages of splenic IFN-α–expressing pDCs and IL-6^+ myeloid cells.

For the measurement of dsDNA-specific Ab titers, ELISA plates were coated with 10 μg/ml salmon testes DNA (Calbiochem, catalog no. 262012) in a Reacti-Bind DNA coating solution (Thermo Scientific, catalog no. 17250) at room temperature overnight. The plates were then washed with PBS and blocked for 60 min with 2% BSA in PBS. Sera samples diluted in assay diluent buffer (2% BSA prepared in PBS with 0.1% Tween 80) were transferred to the plates and incubated for 90 min at room temperature. The bound IgG was detected with goat anti-mouse IgG conjugated with HRP (SouthernBiotech, Birmingham, AL). Total IgG and IgM titers were measured by ELISA. Serum samples were bound to plates and detected with either goat anti-mouse IgG (SouthernBiotech) or goat anti-mouse IgM (SouthernBiotech). Urine NGAL levels, plasma IL-10, and IL-12p40 were measured by commercially available ELISA kits (NGAL, R&D Systems, no. Dy1857; IL-10, R&D Systems, no. DY417; IL-12p40, BD Biosciences, no. 555165). Protein levels in the urine were measured by the Bradford assay. Serum blood urea nitrogen levels were measured using an autoanalyzer (Beckman Coulter). To determine the percentages of splenic IFN-α–expressing pDCs and IL-6^+ myeloid cells, a spleen single-cell suspension was prepared and cells were stained with anti-mouse PDCA-PE in combination with anti-mouse IFN-α–FITC Abs (PBL Assay Science). Separate aliquots of cells were stained for anti-mouse CD11b-FITC in combination with anti-mouse IL-6 PE Abs (BD Biosciences). Sample acquisition was done using a BD FACSCalibur (BD Biosciences), and data were analyzed by FlowJo software (version 8.5.2; Tree Star, Ashland, OR). At the end of study, kidneys were collected for histology and analysis of Ab complex deposition by immunofluorescence. Kidney samples were fixed in 10% neutral buffered formalin, embedded in paraffin, and stained with H&E. Disease severity was evaluated microscopically under three categories. Glomeruli were evaluated for mesangial matrix thickening, crescent formation, infiltration of mononuclear cells, and fibrosis. Kidney tubules were evaluated for necrosis/dilation, inflammatory cell infiltration, and protein cast formation. Tubulointerstitial areas were evaluated for fibrosis and inflammatory cell infiltration. The lesions were scored on the severity scale of 0–4 (0, unremarkable; 1, minimal; 2, mild; 3, moderate; and 4, marked). To determine the IgG complex deposition by immunofluorescence, slides containing 5-μm tissue sections were fixed in acetone and stained using a mixture of FITC-labeled Abs specific for mouse IgG1 (BD Pharmingen, no. 553443), mouse IgG2a (BD Pharmingen, no. 553390), mouse IgG3 (BD Pharmingen, no. 553403), and mouse IgG2a/2b (BD Pharmingen, no. 553399). The intensity of the fluorescence and number of positive glomeruli were quantitated using a fluorescence microscope. Plasma levels of BMS-986126 were determined by liquid chromatography–mass spectrometry.

BMS-986126 was also tested in combination with prednisolone in the MRL/*lpr* model. Male MRL/*lpr* mice (12–14 wk of age, The Jackson Laboratory) were screened and randomized based on titers of anti-dsDNA Abs and urine levels of NGAL. Mice were dosed daily by oral gavage with either 0.3 or 1 mg/kg BMS-986126 alone, 1 or 10 mg/kg prednisolone alone, or the combination of 0.3 mg/kg BMS-986126 plus 1 mg/kg prednisolone or 1 mg/kg BMS-986126 plus 1 mg/kg prednisolone. The control group was dosed daily with vehicle (40% 20 mM citrate buffer, 45% PEG-300, 10% EtOH, 5% Pluronic F-68). After 8 wk of dosing, disease severity end points were assessed, including proteinuria and anti-dsDNA titers. Plasma levels of BMS-986126 were determined by liquid chromatography–mass spectrometry.

NZB/NZW SLE model

Female NZB/NZW mice 12–14 wk of age (The Jackson Laboratory) were screened and randomized based on the titers of anti-dsDNA Abs. Animals were treated orally, once daily for 25 wk with either BMS-986126 at 0.3, 1, 3, or 10 mg/kg/d or dexamethasone at 1 mg/kg/d. Vehicle controls were dosed daily with 40% 20 mM citrate buffer, 45% PEG-300, 10% EtOH, and 5% Pluronic F-68. The effect of BMS-986126 on disease severity was assessed by measuring end points, including urine protein and NGAL levels, anti-dsDNA Ab titers, total IgM and IgG titers, plasma IL-12 p40 levels, and numbers of splenic IFN-α–expressing pDCs as described above. Expression of IFIT1 in peripheral blood was measured using qPCR. RNA was isolated using RNeasy mini kits (Qiagen) and reverse transcribed using iScript reverse transcription supermix for RT-qPCR (Bio-Rad Lab-

oratories, catalog no. 170 8841). qPCR assays for IFIT1 and the housekeeping gene PPIA were performed using SsoFast EvaGreen Supermix (Bio-Rad Laboratories, catalog no. 172 5201). At the end of study, kidneys were collected and analyzed for histology and Ab complex deposition as described above.

Statistical analysis

Statistical tests were performed as described in each figure legend using Graphpad Prism software.

Results

In vitro profile of BMS-986126

BMS-986126 was identified through structure-guided optimization of compounds identified in a kinase-directed chemical screen. This compound potently inhibited IRAK4 kinase activity with an IC_{50} of 5.3 nM (Table I). Furthermore, the compound was >100-fold selective for IRAK4 over a panel of 214 kinases (data not shown). We further confirmed the selectivity of BMS-986126 against an external panel of 338 kinases. When tested in duplicate at a concentration of 1 μM, the only kinase inhibited by >50% was IRAK4 (data not shown). These data demonstrate that BMS-986126 is a potent and highly selective inhibitor of IRAK4.

We confirmed the selectivity of BMS-986126 in a panel of MyD88-dependent and MyD88-independent functional assays using human PBMCs. As shown in Table I, BMS-986126 demonstrated similar potency against multiple MyD88-dependent TLRs, including TLR2, TLR5, TLR7, and TLR9, with IC_{50}s across multiple donors ranging from 135 to 456 nM. The inhibition of TLR2-induced IL-6 production in human and mouse whole blood was comparable and similar to the potencies observed in human PBMCs (Table I). In addition to triggering NF-κB and AP-1 activation, TLR7 and TLR9 also activate IRF7, resulting in production of type I IFNs (1). BMS-986126 inhibited production of both an NF-κB–regulated protein (IL-6) and type I IFN (IFN-α) with similar potency following stimulation with a TLR7 agonist (Table I). The compound potency for inhibition of TLR9-induced IFN-α was also similar to that for TLR7 stimulation. The other class of receptors that uses MyD88 and IRAK4 for signaling is the IL-1 family. BMS-986126 inhibited cytokine production induced by IL-1β and by IL-18 with similar potency to that observed in the other MyD88-dependent TLR assays (Table I). Unexpectedly, we observed very little inhibition of TLR4-induced IL-6 production. This suggests that TLR4 may use the IRAK4-independent, TIR domain–containing adaptor-inducing IFN-β (TRIF)-dependent pathway to induce IL-6 production. Consistent with the selectivity profile of the compound, BMS-986126 failed to significantly inhibit cytokine production induced either by a TLR3 agonist or by TNF-α (Table I).

Although BMS-986126 did not inhibit LPS-induced cytokine production, we did see inhibition of IKKα/β phosphorylation (Fig. 1A), a response that has been shown to be dependent on IRAK4 kinase activity (13). We also saw inhibition of LPS-induced ERK phosphorylation that is farther downstream in the signaling cascade. Consistent with the inhibition of cytokine production, BMS-986126 inhibited TLR2-induced IKKα/β and ERK phosphorylation (k. 1B). Although we were unable to detect robust IKKα/β phosphorylation in response to the TLR7 agonist gardiquimod (data not shown), BMS-986126 did robustly inhibit gardiquimod-induced ERK phosphorylation (Fig. 1C).

In vivo efficacy of BMS-986126

To determine the impact of IRAK4 inhibition in vivo, we first assessed the activity against different TLR-dependent pharmacodynamic responses in mice. Mice were dosed orally with vehicle or BMS-986126 followed by challenge with either the TLR2 agonist LTA, the TLR9 agonist ODN2216, or the TLR7 agonist gardiquimod (Fig. 2). Cytokine levels were measured 90 min after LTA challenge, which was determined to be the peak response in a prior kinetic study. Cytokine levels drop rapidly in control animals after 2 h after LTA challenge (data not shown). BMS-986126 dose-dependently suppressed LTA-induced IL-6 plasma levels, with maximal inhibition observed at the top dose of 3 mg/kg (Fig. 2A). We measured IFN-α in the plasma at 2, 8, and 24 h after challenge with the TLR9 agonist CpG oligonucleotide (Fig. 2B). BMS-986126 strongly suppressed IFN-α at both 2 and 8 h after challenge. No IFN-α was detected in any group at 24 h after challenge (data not shown). Lastly, we looked at cytokine production at 2, 8, and 24 h after challenge with the TLR7 agonist gardiquimod (Fig. 2C, 2D). BMS-986126 dose-dependently suppressed both IFN-α (Fig. 2C) and IL-6 production (Fig. 2D) at both 2 and 8 h after challenge. Both cytokines were below the limit of detection at the 24 h time point (data not shown). Although there was less suppression of gardiquimod-induced cytokines at the 1 mg/kg dose as compared with the other TLR agonists, this could be due to the very robust cytokine responses induced by gardiquimod. Overall, we conclude that these results are consistent with the activity observed in human PBMCs, indicating that BMS-986126 inhibits multiple MyD88-dependent TLR responses.

The endosomal TLRs, TLR7 and TLR9, have been implicated in several diseases, including psoriasis and lupus (19). To assess the role of IRAK4 in TLR7-induced skin inflammation, we induced psoriasis-like symptoms with daily topical application of the TLR7 agonist imiquimod for 6 d. Daily treatment with BMS-986126 dose-dependently suppressed skin thickening (Fig. 3A), scaling (Fig. 3B), erythema (Fig. 3C), and spleen weight gain

Table I. Potency of BMS-986126 in TLR-, IL-1β–, IL-18–, and TNF-α–induced cytokine assays

Assay	Receptor (Stimulus)	IC_{50} (nM)
PBMC TLR2-induced IL-6	TLR2 (LTA)	333 ± 96, *n* = 5
PBMC TLR5-induced IL-6	TLR5 (flagellin)	135 ± 26, *n* = 3
PBMC TLR7-induced IL-6	TLR7 (gardiquimod)	456 ± 362, *n* = 4
PBMC TLR7-induced IFN-α	TLR7 (gardiquimod)	353 ± 19, *n* = 3
PBMC TLR9-induced IFN-α	TLR9 (ODN2216)	187 ± 121, *n* = 3
PBMC TLR4-induced IL-6	TLR4 (LPS)	>10,000, *n* = 3
PBMC TLR3-induced IP-10	TLR3 [poly(I:C)]	>10,000; 4,300
PBMC IL-1–induced IL-8	IL-1R (IL-1β)	267 ± 272, *n* = 3
PBMC IL-18 plus IL-12–induced IFN-γ	IL-18 plus IL-12	418 ± 267, *n* = 3
PBMC TNF-α–induced IL-8	TNFR (TNF-α)	>10,000; 6,340
Human whole blood TLR2-induced IL-6	TLR2 (LTA)	414 ± 497, *n* = 8
Mouse whole blood TLR2-induced IL-6	TLR2 (LTA)	380 ± 83, *n* = 4

Values represent mean IC_{50} ± SD of three to eight independent donors.

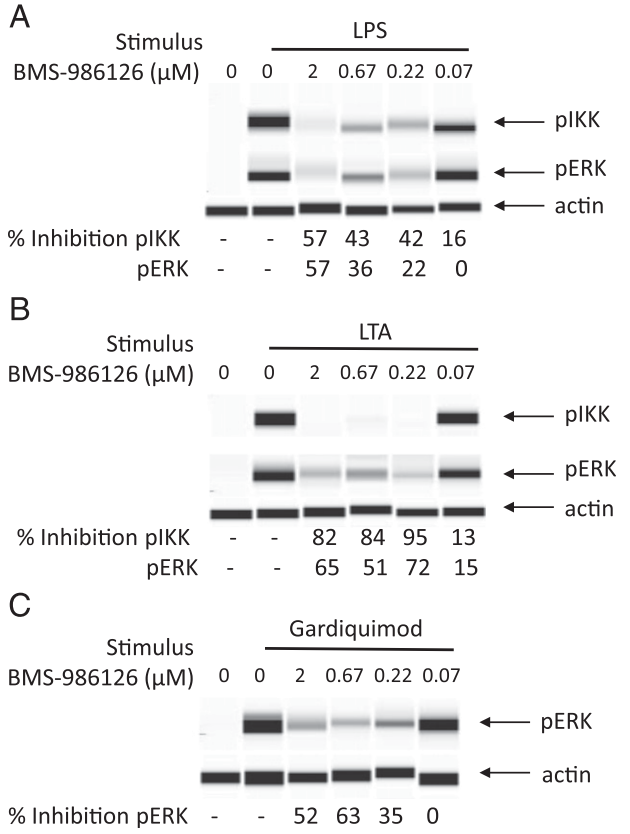

FIGURE 1. Inhibition of TLR-induced IKKα/β and ERK phosphorylation by BMS-986126. PBMCs were cultured with different concentrations of BMS-986126 and stimulated with either 100 ng/ml LPS (**A**) or 10 μg/ml LTA (**B**) for 20 min. Some groups were stimulated with 10 μg/ml gardiquimod for 30 min (**C**). Lysates were analyzed using the Sally Sue ProteinSimple system. The pIKKα/β and pERK bands were normalized to actin bands for each group. Percentage inhibition relative to the vehicle control is shown under each band. Cropped bands for pIKKα/β, pERK, and actin are shown. One representative experiment of two is shown.

(Fig. 3D). The highest two doses of 3 and 10 mg/kg/d also significantly inhibited skin histopathology (Fig. 3E). At the 10 mg/kg/d dose, plasma levels of BMS-986126 were maintained above the mouse in vitro whole blood LTA-induced IL-6 IC_{50} value for 24 h (data not shown), consistent with complete suppression of IRAK4 activity. However, doses as low as 1 mg/kg/d suppressed many end points. At this dose, compound concentrations were maintained above the mouse whole blood IC_{50} value (LTA-induced IL-6 IC_{50}) for 8–12 h out of the day (data not shown), suggesting that partial inhibition of IRAK4 activity can have benefit in this model.

TLR7 has been shown to contribute to pathology in the MRL/*lpr* mouse model of lupus (20). Given the strong efficacy we saw with BMS-986126 in the imiquimod-induced skin inflammation model, we tested the compound in the MRL/*lpr* model. Daily dosing was initiated when mice were 12–14 wk of age with detectable levels of dsDNA-specific autoantibodies in the sera. Following 8 wk of daily dosing, BMS-986126 dose-dependently suppressed biomarkers of kidney damage and systemic inflammation. We observed very strong inhibition of kidney damage end points, including reduction of absolute protein levels in the urine (Fig. 4A), urine NGAL levels (Fig. 4B), and serum blood urea nitrogen (Fig. 4C). Urine NGAL has been used as a biomarker of kidney damage in lupus nephritis patients (21). Doses of BMS-986126 as low as 1 mg/kg/d demonstrated significant protection of all end points. The highest dose of 10 mg/kg/d matched the level of efficacy achieved with a 10 mg/kg dose of prednisolone for these end points. BMS-986126 also dose-dependently suppressed dsDNA-specific autoantibody titers (Fig. 4D), as well as plasma levels of IL-10 (Fig. 4E) and IL-12p40 (Fig. 4F). Consistent with the role of TLR7 and TLR9 in induction of IFN-α production by pDCs, BMS-986126 significantly suppressed the percentage of splenic IFN-α^+ pDCs at both the 1 and 10 mg/kg doses (Fig. 4G, Supplemental Fig. 1A). BMS-986126 also suppressed IL-6 production by splenic $CD11b^+$ myeloid cells (Fig. 4H, Supplemental Fig. 1A), suggesting that this response could be driven by MyD88-dependent pathways, either TLRs or IL-1 family cytokines. Compound treatment had no effect on total numbers of splenic lymphocytes and myeloid cells, or total levels of serum IgM and IgG (Supplemental Fig. 1B, 1C). Although the highest dose of 10 mg/kg approached the level of inhibition achieved with 10 mg of prednisolone, the lower doses of BMS-986126 were less effective against these systemic end points. Consistent with the inhibition of serum autoantibody titers, all but the lowest dose inhibited IgG deposition in the kidney (Fig. 4I). Lastly, BMS-986126 also dose-dependently suppressed histopathology in the kidney (Fig. 4J, 4K). These data suggest that IRAK4-dependent signaling contributes to both tissue and systemic pathology in the MRL/*lpr* model.

To confirm the benefit of IRAK4 inhibition beyond the MRL/*lpr* model, we also tested BMS-986126 in the NZB/NZW model of lupus. Daily dosing was initiated when mice were 12–14 wk of age with detectable levels of urine NGAL and plasma dsDNA-specific autoantibody titers. Following 25 wk of dosing, BMS-986126 strongly suppressed biomarkers of kidney damage at all doses tested, including urine protein levels (Fig. 5A) and urine levels of NGAL (Fig. 5B). BMS-986126 suppressed these end points to a similar extent as that achieved with a 1 mg/kg dose of dexamethasone. Systemic end points including dsDNA-specific autoantibody titers (Fig. 5C) and plasma IL-12p40 levels (Fig. 5D) were also dose-dependently suppressed. Consistent with the importance of TLR7 and TLR9 in IFN-α production by pDCs, BMS-986126 inhibited the percentage of splenic IFN-α^+ pDCs as measured by flow cytometry (Fig. 5E, Supplemental Fig. 2A). Compound dosing did not impact total splenic B cell and myeloid cell percentages, or serum levels of total IgM and IgG (Supplemental Fig. 2B, 2C). Expression of the IFN response gene IFIT1 in peripheral blood was also significantly inhibited (Fig. 5F). As seen in the MRL/*lpr* model, BMS-986126 dose-dependently inhibited Ig deposition in the kidney (Fig. 5G). Consistent with the inhibition of multiple disease-associated biomarkers, BMS-986126 significantly suppressed histopathology in the kidneys of these animals with profound effects on glomerular damage and tubular damage subscores (Fig. 5H, 5I).

Inhibition of TLR7- and TLR9-induced IFN response genes in healthy controls and lupus samples

The robust efficacy of BMS-986126 in two different lupus models suggested that IRAK4 inhibition is a viable approach for therapeutic intervention in lupus patients. One characteristic of most lupus patients is the overexpression of IFN-regulated genes in peripheral blood leukocytes. This induction is thought to partially derive from TLR7 and TLR9 signaling in pDCs. As shown in Table I, BMS-986126 potently inhibited TLR7- and TLR9-induced IFN-α production by human PBMCs. To confirm that the compound also impacted expression of IFN-regulated genes, we measured the inhibition of TLR7- and TLR9-induced expression of two canonical IFN-regulated genes, IFIT1 and MX1. As shown in Fig. 6, BMS-986126 potently inhibited expression of IFIT1 (Fig. 6A) and MX1 (Fig. 6B) following stimulation with TLR7 agonists, including gardiquimod and attenuated influenza

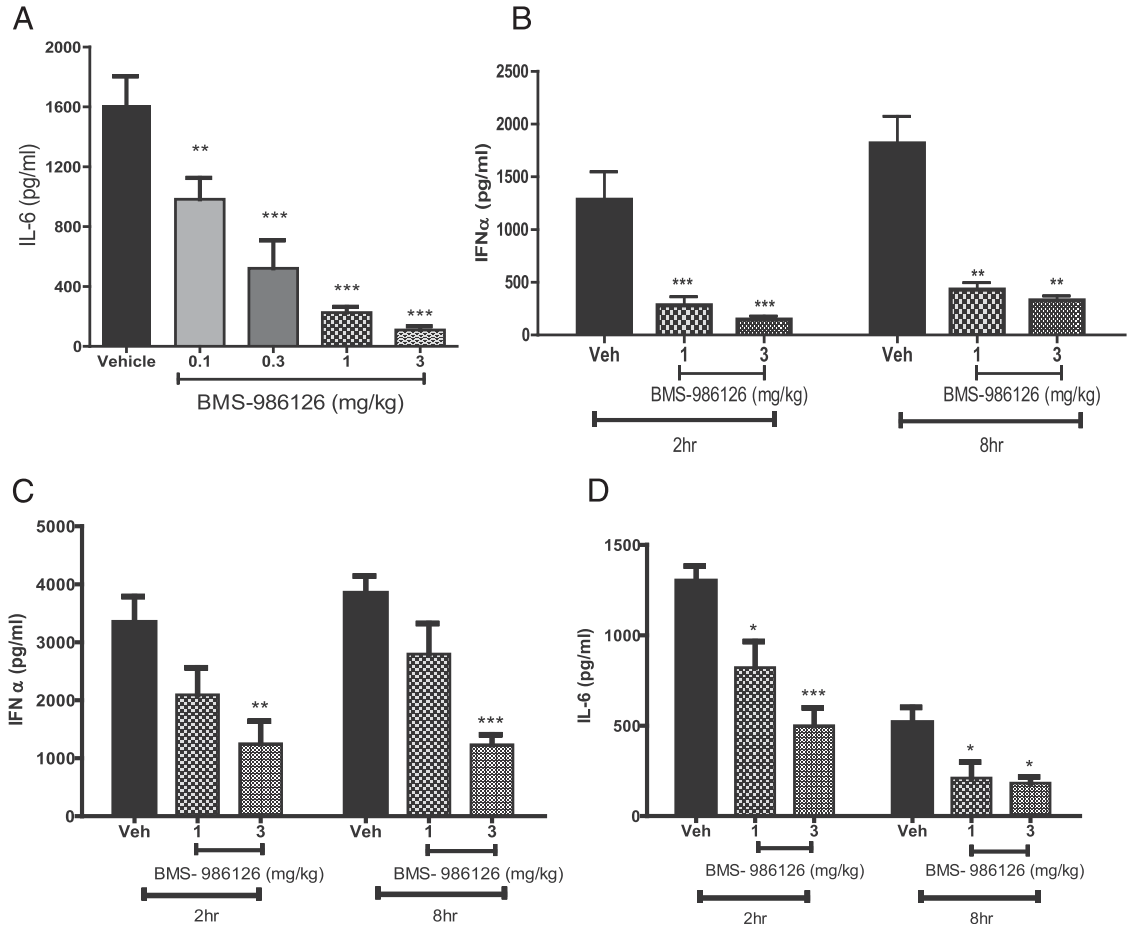

FIGURE 2. Inhibition of TLR-induced cytokines by BMS-986126 in mice. Mice were dosed orally with either vehicle or the indicated doses of BMS-986126 at 30 min prior to challenge either with 25 mg/kg LTA i.p. (**A**), 2.5 μg CpG-ODN i.v. (**B**), or 5 mg/kg gardiquimod i.p (**C** and **D**). Ninety minutes after LTA challenge, mice were bled and plasma concentrations of IL-6 were determined by ELISA. Mice were bled 2 and 8 h after CpG challenge, and plasma levels of IFN-α were measured by ELISA. Plasma concentrations of IFN-α (C) and IL-6 (D) were measured at 2 and 8 h after challenge with gardiquimod. Mean and SEM are plotted. Data are from one experiment with eight animals per group. $^{**}p < 0.001$, $^{***}p < 0.0001$, one-way ANOVA with a Dunnett test.

virus, as well as the TLR9 agonist ODN2216. The potency of the compound was similar comparing PBMCs derived from healthy controls to those from lupus patients (Fig. 6C). We confirmed that BMS-986126 impacted gene expression beyond these selected genes by performing broader transcriptomic profiling of gardiquimod-induced genes in human PBMCs using Affymetrix profiling. As shown in Fig. 6D, most gardiquimod-induced genes were inhibited by BMS-986126. Many of these genes are canonical IFN-regulated genes (Supplemental Table I). Lastly, we confirmed that BMS-986126 also inhibited expression of IFN-regulated genes induced by a disease-relevant stimulus, anti-RNP autoantibodies purified from lupus plasma (Fig. 6E). We mixed necrotic cell lysate as a source of Ag with the RNP-specific IgG purified from lupus patients, and used the complex to stimulate PBMCs from three different donors. The autoantibody complex stimulated robust expression of IFIT1 message. This stimulation was completely blocked by BMS-986126 with a potency that matched the activity in assays using synthetic TLR7 and TLR9 agonists.

Steroid sparing activity of BMS-986126

One of the unmet medical needs in lupus is for therapies that can decrease the need for high-dose steroids. It has been shown that TLR7- and TLR9-dependent signaling antagonizes glucocorticoid-dependent apoptosis of pDCs (22). It was also shown that blockade of TLR7 and TLR9 signaling enhances the efficacy of steroids. We tested whether the combination of IRAK4 inhibition with glucocorticoids would show enhanced activity in comparison with either agent alone. In vitro, the combination of suboptimal concentrations of BMS-986126 with suboptimal concentrations of prednisolone demonstrated increased inhibition of TLR9-induced (Fig. 7A) and flu virus–induced (Fig. 7B) IFIT1 expression as compared with either agent alone. Similar results were obtained for induction of MX1 (data not shown). We also tested the combination of suboptimal doses of BMS-986126 (0.3, 1 mg/kg) with a suboptimal dose of prednisolone (1 mg/kg) in the MRL/*lpr* mouse lupus model. Doses of 0.3 mg/kg BMS-986126 and 1 mg/kg prednisolone partially suppressed dsDNA-specific Ab titers (Fig. 7C) and proteinuria (Fig. 7D), but they showed enhanced efficacy when combined together. The degree of proteinuria suppression reached the same levels achieved with a 10-fold higher dose of prednisolone, suggesting that IRAK4 inhibition has the potential to provide steroid sparing activity.

Discussion

In this study, we comprehensively profiled a highly selective IRAK4 inhibitor and to our knowledge provide the first description of the impact of IRAK4 inhibition in mouse models of lupus. Consistent with the selectivity profile of BMS-986126, the compound inhibited multiple MyD88-dependent responses with similar potency and demonstrated no activity against agonists that do not use the MyD88 pathway. BMS-986126 also inhibited multiple MyD88-dependent

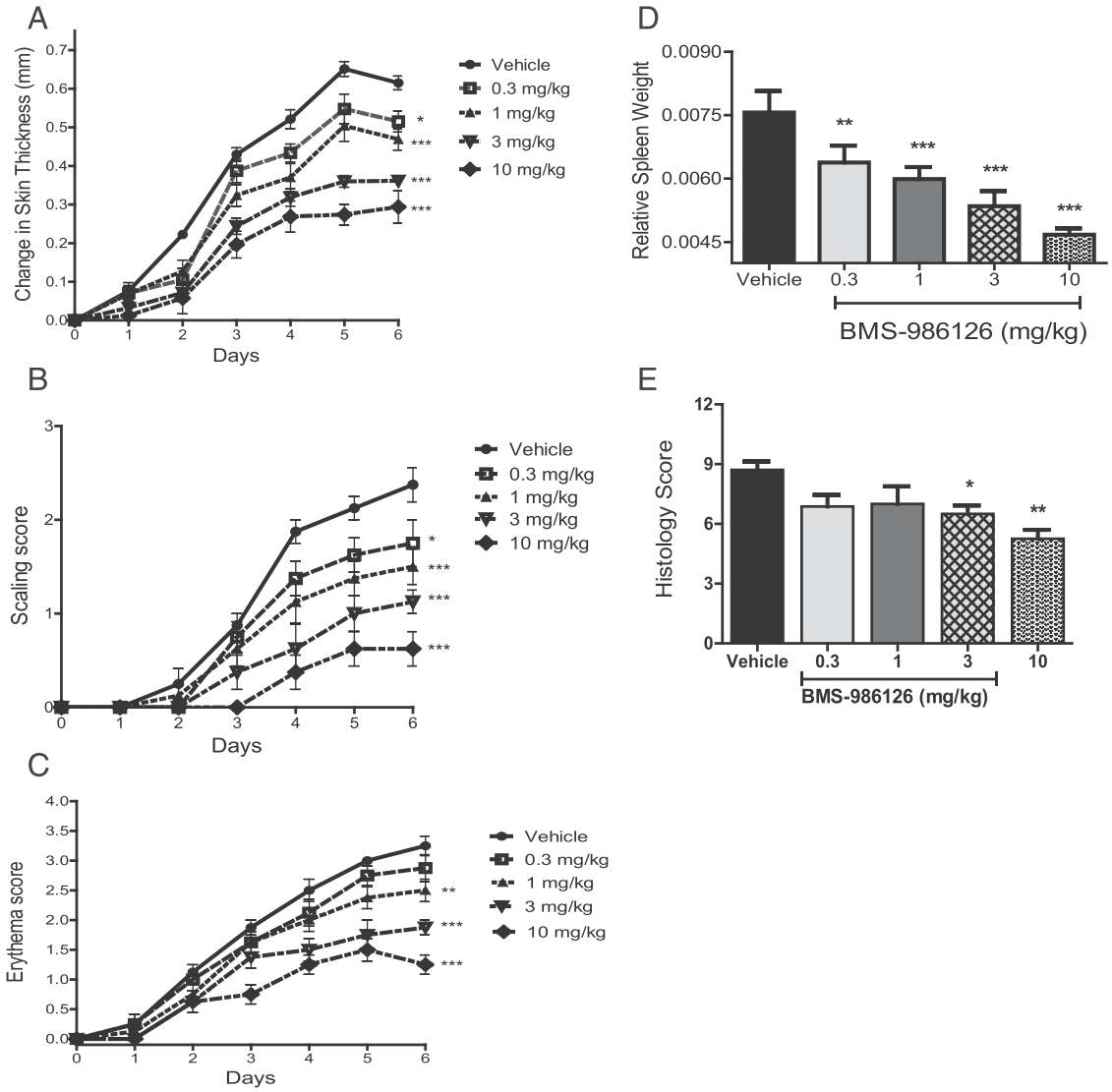

FIGURE 3. Inhibition of TLR7-induced skin inflammation by BMS-986126. C57BL/6 mice were dosed orally with vehicle or BMS-986126 at doses of 0.3, 1, 3, and 10 mg/kg/d. Imiquimod cream was applied daily on the shaved backs of the mice. Changes in skin thickness (**A**), scaling (**B**), and erythema (**C**) were monitored daily. At termination of the study, splenomegaly was assessed by spleen weight normalized by body weight (**D**). Skin histology (**E**) was also assessed at end of study. For (A)–(C), difference from vehicle at day 6 was assessed by two-way ANOVA with the Bonferroni test. For (D) and (E), difference from vehicle on day 6 was assessed by one-way ANOVA with a Dunnett test. Means and SEM for each group are plotted. Data are from one experiment with eight animals per group. $*p < 0.01$, $**p < 0.01$, $***p < 0.0001$.

responses in mice; that is, blocking TLR2-induced IL-6, TLR9-induced IFN-α, TLR7-induced IL-6 and IFN-α, as well as TLR7-induced skin inflammation. Although it has been suggested that human macrophages are less dependent on IRAK4 kinase activity for TLR-dependent responses as compared with mouse macrophages (23), our data do not support species-specific differences in IRAK4 dependence. We observed potent inhibition of most MyD88-dependent responses in human PBMCs with a compound that is highly selective for IRAK4 and lacks any activity against IRAK1. The potency was also similar to that observed using mouse cells. The evidence suggesting TLR signaling in human cells is less dependent on IRAK4 comes primarily from RNA interference and overexpression systems. In contrast, our data derive entirely from assays using primary human lymphocytes across multiple donors.

The activity profile of BMS-986126 is generally consistent with the data described for the IRAK4 KDKI mice and the profiles of human patients lacking expression of IRAK4. The only exception is the impact on TLR4-dependent responses. Although BMS-986126 potently blocked LPS-induced IKKα/β phosphorylation in human PBMCs, we failed to detect significant inhibition of cytokine production. Some residual responses to LPS have been observed in IRAK4 KDKI mice (24) as well as in IRAK4-deficient patients (6). Several IRAK4 inhibitors have been disclosed with activity against LPS-induced cytokines, but this activity could be due to off-target kinase activity (25–27). TLR4 is unique in that it activates two distinct signaling cascades, one dependent on MyD88 and the other dependent on the TRIF adaptor protein. The TRIF-dependent pathway has mainly been associated with type I IFN responses (28). However, it was shown that knockdown of TRIF protein in human immature DCs significantly suppressed LPS/IFN-γ–induced proinflammatory cytokine production (29). Our data suggest that IRAK4 kinase activity regulates some signaling downstream of TLR4, but is not required for proinflammatory cytokine production. The data further suggest that the TRIF pathway may play a more dominant role in regulating these responses in human cells.

Although dysregulated signaling via MyD88-dependent receptors, including TLR7 and TLR9, has been implicated in the

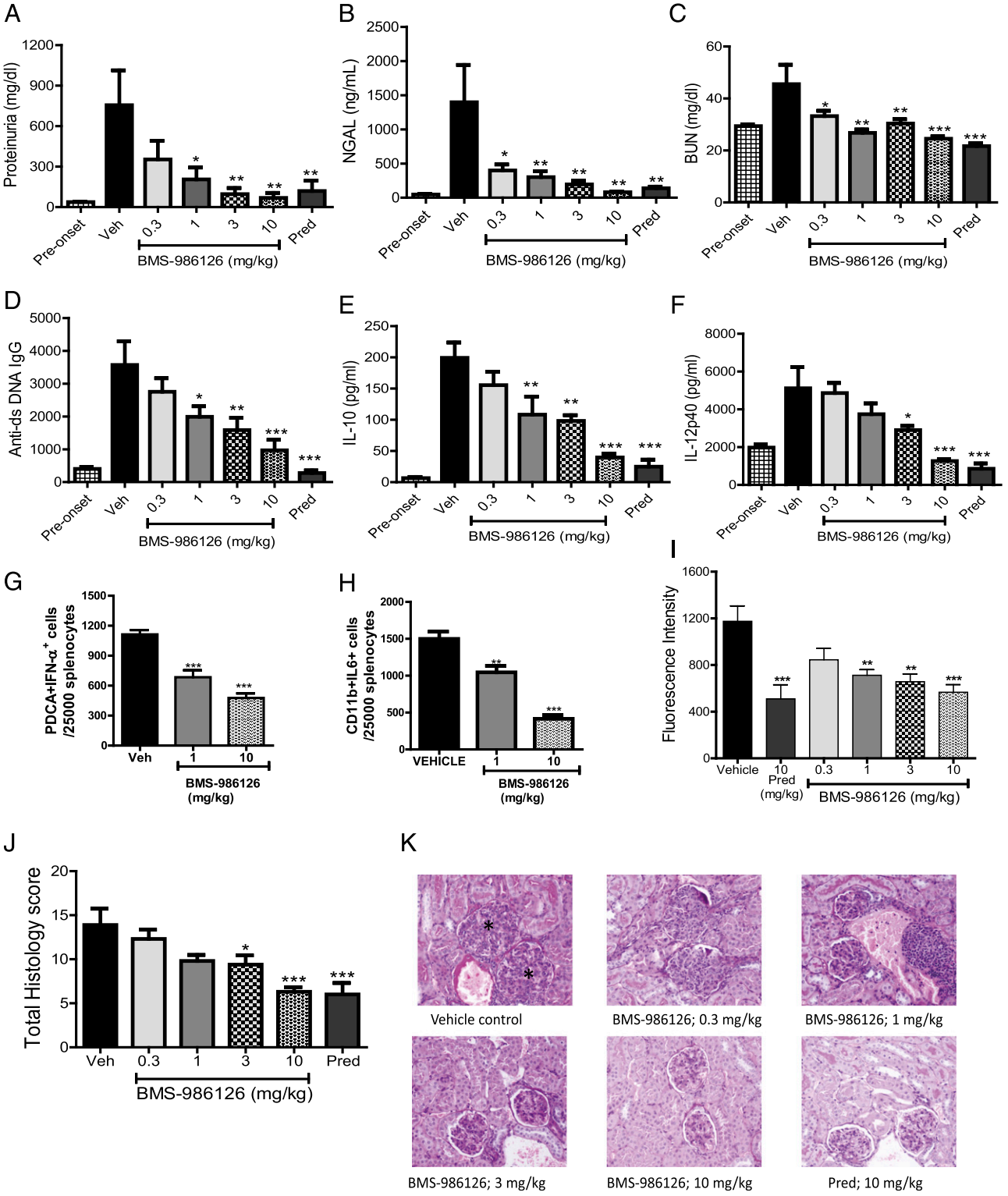

FIGURE 4. Inhibition of disease activity in MRL/*lpr* mice by BMS-986126. Mice were dosed orally either with vehicle or 0.3, 1, 3, or 10 mg/kg/d BMS-986126, or with 10 mg/kg/d prednisolone. Following 8 wk of dosing, multiple biomarkers were assessed, including total urine protein levels (**A**), urine NGAL concentrations (**B**), blood urea nitrogen concentrations (**C**), anti-dsDNA Ab titers (**D**), plasma IL-10 concentrations (**E**), and plasma IL-12p40 concentrations (**F**). In the spleen, the numbers of IFN-α^+ pDCs (**G**) and IL-6^+ myeloid cells (**H**) were determined by flow cytometry. Intensity of Ig deposition in the kidney (**I**) and kidney histology as visualized by H&E staining with ×20 magnification (**J** and **K**) were also assessed at the end of study. Asterisks indicate glomerular changes characterized by mesangial thickening, cellular infiltration, and sclerosis/fibrosis. Preonset values are from MRL/*lpr* mice at 8 wk of age. Means and SEM for each group are plotted. Data are from one experiment with 10 animals per group. *$p < 0.01$, **$p < 0.001$, ***$p < 0.0001$ versus vehicle by one-way ANOVA with a Dunnett test.

pathophysiology of lupus, many of these data derive from genetic knockouts (20). Some efficacy was reported in spontaneous mouse lupus models with oligonucleotide-based antagonists of TLR7, 8, and 9; however, limited end points were described (30, 31). We describe robust efficacy in two different mouse models of lupus and provide detailed dose response information for multiple disease-associated end points. These data provide valuable insights into the pathology most closely linked to IRAK4-dependent

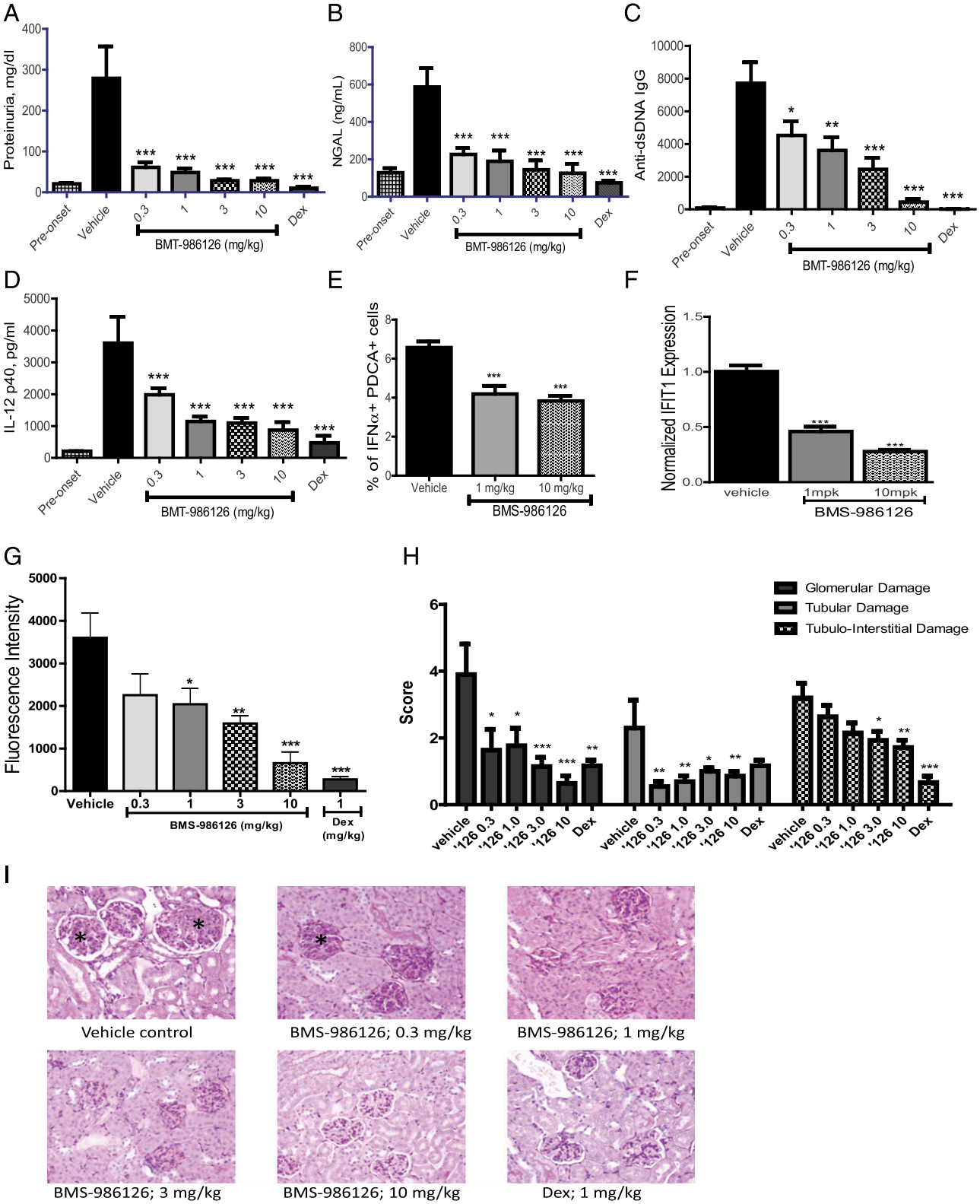

FIGURE 5. Inhibition of disease activity in NZB/NZW mice by BMS-986126. Mice were dosed orally with vehicle or 0.3, 1, 3, or 10 mg/kg/d BMS-986126, or with 1 mg/kg/d dexamethasone (DEX). Following 25 wk of dosing, several biomarkers of disease activity were assessed, including protein (**A**) and NGAL (**B**) concentrations in urine, plasma titers of dsDNA-specific autoantibodies (**C**), plasma levels of IL-12p40 (**D**), numbers of splenic IFN-α^+ pDCs (**E**), expression of IFIT1 mRNA in blood (**F**), intensity of Ig deposition in the kidney (**G**), and kidney histology as visualized by H&E staining with $\times$20 magnification (**H** and **I**). Asterisks indicate glomerular changes characterized by mesangial thickening, cellular infiltration, and sclerosis/fibrosis. Preonset values are from NZB/NZW mice at 10 wk of age. Means and SEM for each group are plotted. Data are from one experiment with 14 animals per group. *$p < 0.01$, **$p < 0.001$, ***$p < 0.0001$ versus vehicle by one-way ANOVA with a Dunnett test.

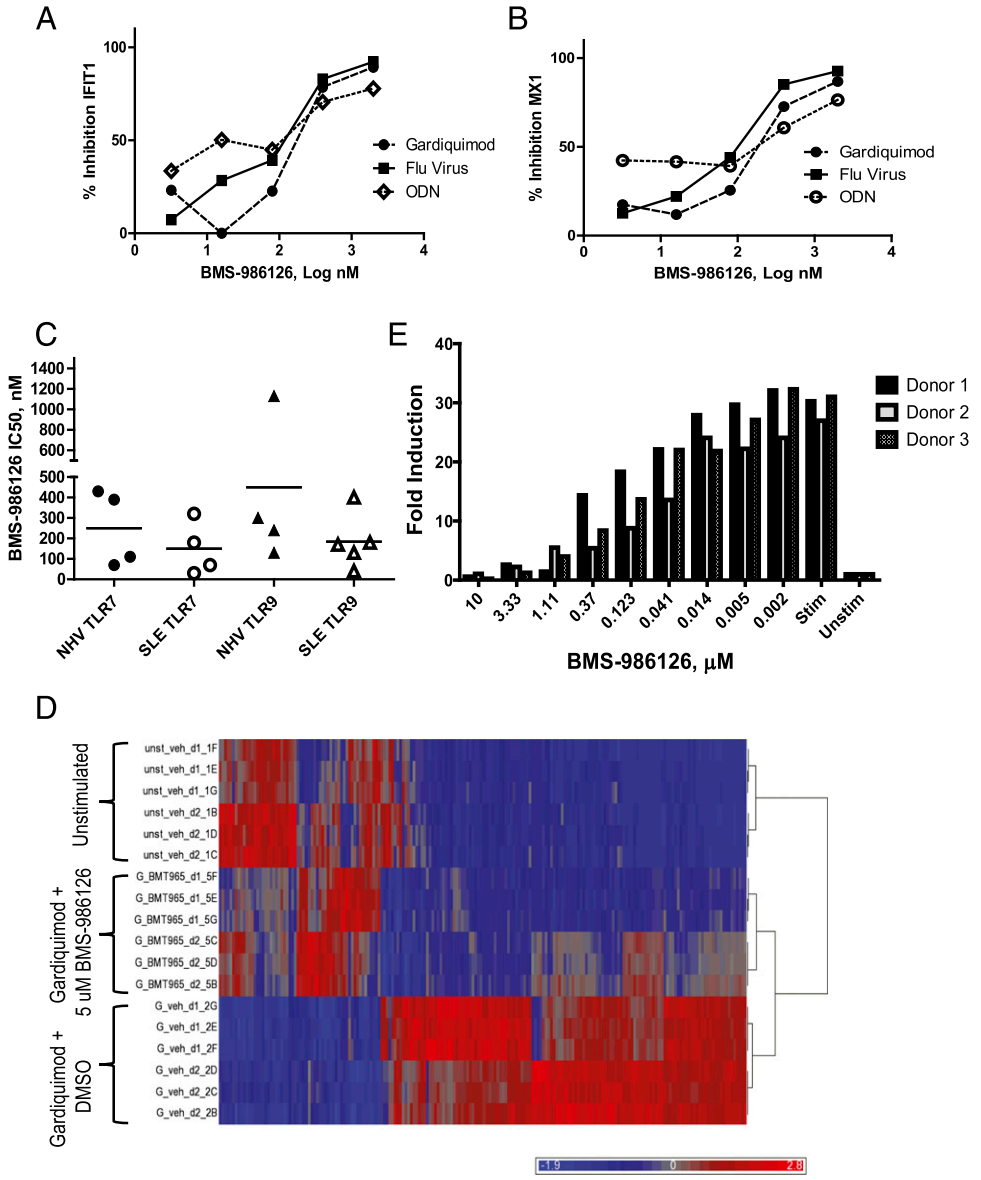

FIGURE 6. Inhibition of TLR7- and TLR9-induced gene expression by BMS-986126. PBMCs were stimulated in duplicate with the TLR7 agonists gardiquimod (0.5 μg/ml) and heat-inactivated influenza virus (0.02 μl) or the TLR9 agonist ODN2216 (300 nM) in the presence and absence of different concentrations of BMS-986126. Expression of the target genes IFIT1 (**A**) and MX1 (**B**) were measured by qPCR, normalized to the housekeeping gene GAPDH, and compared with unstimulated levels to determine fold induction. Data are expressed as percentage inhibition of fold induction relative to a DMSO control for one representative donor of three. (**C**) PBMCs from either healthy controls (NHV) or lupus patients (SLE) were stimulated with either a TLR7 agonist (gardiquimod, 0.5 μg/ml) or a TLR9 agonist (ODN2216, 300 nM) in the presence and absence of BMS-986126. The IC_{50}s for compound-dependent inhibition of IFIT1 from four to five independent donors are plotted. (**D**) Heat map of PBMCs from two donors stimulated in triplicate with gardiquimod (5 μg/ml) in the presence and absence of 5 μM BMS-986126. The top 196 genes significantly inhibited by BMS-986126 in both donors are shown. (**E**) PBMCs from three healthy controls were stimulated with a complex of anti-RNP Abs purified from lupus patients mixed with necrotic cell lysates in the presence and absence of BMS-986126. Fold induction of normalized IFIT1 expression is plotted. One representative experiment of three is shown.

regulation. Consistent with the importance of TLR7 and TLR9 in B cell–driven responses, BMS-986126 dose-dependently suppressed dsDNA-specific autoantibody titers as well as Ig deposition in the kidney. Several cytokines were also suppressed, including IL-10 and IL-12. In the spleen, the compound suppressed IL-6–producing $CD11b^+$ myeloid cells and IFN-α–producing pDCs. The latter is consistent with the role of TLR7 and TLR9 in stimulating IFN-α production. Additional MyD88-dependent pathways may also play a role in the systemic production of proinflammatory cytokines. MyD88 deletion in DCs on the MRL/*lpr* background was shown to impair both IFN-α production by pDCs as well as expression of proinflammatory cytokines, including IL-6 (32). In addition to inhibiting TLR-dependent responses, BMS-986126 also blocked cytokine production induced by IL-1β and IL-18. In both the MRL/*lpr* and NZB/NZW models, we observed more profound suppression of several kidney damage markers, including proteinuria, blood urea nitrogen, and urine NGAL levels relative to systemic biomarkers such as dsDNA titers. At the level of histology, glomerular damage was more significantly suppressed relative to tubulointerstitial and tubular end points. In addition to expression on infiltrating lymphoid and myeloid cells, TLRs are expressed by several kidney-resident cell populations, including podocytes (33). These cells may respond to any damage-associated molecular pattern molecules released in response to tissue damage (34). The IL-1 and IL-18 pathways may also contribute to renal damage. Expression of the inflammasome component NLRP3 as

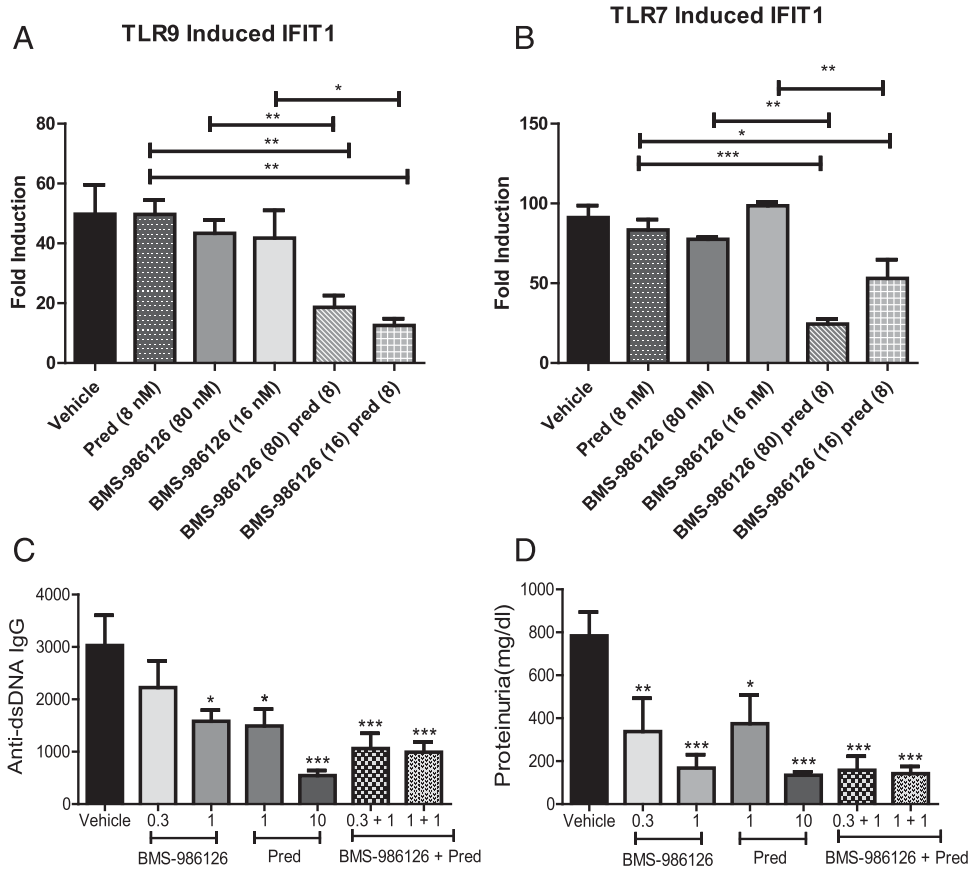

FIGURE 7. Synergistic inhibition of TLR7- and TLR9-induced IFN-regulated genes by the combination of BMS-986126 and prednisolone. PBMCs from a healthy control donor were stimulated in vitro either with the TLR9 agonist ODN2216 (300 nM) (**A**) or the TLR7 agonist heat-inactivated influenza virus (0.02 μl) (**B**) in the presence and absence of suboptimal concentrations of prednisolone, BMS-986126, and the combination of both. Expression of IFIT1 was quantitated by real-time PCR and normalized to the housekeeping gene GAPDH. Data represent fold induction relative to unstimulated controls. One representative experiment of three is shown. Comparisons were performed as shown using a one-way Student *t* test. $*p < 0.01$, $**p < 0.001$, $***p < 0.0001$. (**C** and **D**) MRL/*lpr* mice were dosed orally with suboptimal doses of BMS-986126 (0.3 or 1 mg/kg/d), two doses of prednisolone (pred, 1 or 10 mg/kg/d), or the combination of BMS-986126 with prednisolone (0.3 + 1; 1 + 1). Following 8 wk of dosing, serum titers of dsDNA-specific autoantibodies (C) and urine protein levels (D) were measured. Mean and SEM for each group are plotted. Data are from one experiment with 10 animals per group. $*p < 0.01$, $**p < 0.001$, $***p < 0.0001$ versus vehicle by one way ANOVA with Dunnett's test.

well as mature IL-1β and IL-18 were shown to be elevated in kidney tissue from NZB/NZW mice. Treatment with an antioxidant suppressed IL-1β and IL-18 expression and was associated with reduced proteinuria and improved kidney histology (35). Renal-protective effects of an IRAK4 inhibitor in a rat chronic kidney model (five of six nephrectomized rats) have been described (27). Our data are also consistent with a recent report demonstrating that expression of catalytically inactive IRAK4 provided protection from kidney inflammation and autoimmunity in a mouse strain expressing a mutant form of A20-binding inhibitor of NF-kB1. This strain develops pathology similar to human lupus nephritis (36).

The robust efficacy in animal models of lupus suggests that IRAK4 inhibition has the potential to provide therapeutic benefit in lupus patients. To begin to translate to human disease, we confirmed that BMS-986126 inhibited TLR7- and TLR9-induced expression of IFN response genes, both in healthy controls and lupus patients. Although we focused on two IFN response genes to assess the compound potency, we confirmed that BMS-986126 inhibited TLR7-induced gene expression more broadly by using Affymetrix arrays. These experiments were performed using synthetic agonists of TLR7 and TLR9. We also tested a disease-relevant stimulus, nucleic acid–containing immune complex. Culturing cells with an RNP-specific Ab mixed with necrotic cell lysate induced robust expression of IFN-regulated genes. This response was potently blocked by BMS-986126. Blockade of the IFN receptor was recently shown to provide clinical benefit to lupus patients in a phase II study (37), indicating that this pathway contributes to pathology in human disease.

One of the major unmet needs in lupus is a therapeutic that can reduce steroid doses. Many lupus patients require very high doses of steroids to maintain disease control. It was demonstrated that signaling through TLR7 and TLR9 in human pDCs contributes to the reduced efficacy of glucocorticoids in suppressing the IFN pathway in lupus patients (22). We demonstrated that suboptimal concentrations of prednisolone and BMS-986126 synergized to significantly suppress TLR7- and TLR9-induced expression of IFN-regulated genes in vitro. We also saw enhanced efficacy with the combination of suboptimal doses of each compound in the MRL/*lpr* model. These data further support the compelling profile of IRAK4 inhibition for the treatment of lupus. Although patients lacking IRAK4 expression are at increased risk for severe infections in childhood, this risk has been shown to decrease in adulthood (38). We suggest that inhibition of IRAK4 may provide a new approach for the treatment of adult patients with lupus and potentially other autoimmune diseases.

Disclosures

All of the authors are either employees of or are affiliated with Bristol-Myers Squibb. J.A.C., J.H., J.D., X.L., S. Ruepp, D.A.H., and L.F. have stock in Bristol-Myers Squibb.

References

1. Kawai, T., and S. Akira. 2010. The role of pattern-recognition receptors in innate immunity: update on Toll-like receptors. *Nat. Immunol.* 11: 373–384.
2. Sims, J. E., and D. E. Smith. 2010. The IL-1 family: regulators of immunity. *Nat. Rev. Immunol.* 10: 89–102.
3. Lin, S. C., Y. C. Lo, and H. Wu. 2010. Helical assembly in the MyD88-IRAK4-IRAK2 complex in TLR/IL-1R signalling. *Nature* 465: 885–890.
4. Flannery, S., and A. G. Bowie. 2010. The interleukin-1 receptor-associated kinases: critical regulators of innate immune signalling. *Biochem. Pharmacol.* 80: 1981–1991.
5. Picard, C., A. Puel, M. Bonnet, C. L. Ku, J. Bustamante, K. Yang, C. Soudais, S. Dupuis, J. Feinberg, C. Fieschi, et al. 2003. Pyogenic bacterial infections in humans with IRAK-4 deficiency. *Science* 299: 2076–2079.
6. Ku, C. L., H. von Bernuth, C. Picard, S. Y. Zhang, H. H. Chang, K. Yang, M. Chrabieh, A. C. Issekutz, C. K. Cunningham, J. Gallin, et al. 2007. Selective predisposition to bacterial infections in IRAK-4-deficient children: IRAK-4-dependent TLRs are otherwise redundant in protective immunity. *J. Exp. Med.* 204: 2407–2422.
7. Suzuki, N., S. Suzuki, G. S. Duncan, D. G. Millar, T. Wada, C. Mirtsos, H. Takada, A. Wakeham, A. Itie, S. Li, et al. 2002. Severe impairment of interleukin-1 and Toll-like receptor signalling in mice lacking IRAK-4. *Nature* 416: 750–756.
8. Thomas, J. A., J. L. Allen, M. Tsen, T. Dubnicoff, J. Danao, X. C. Liao, Z. Cao, and S. A. Wasserman. 1999. Impaired cytokine signaling in mice lacking the IL-1 receptor-associated kinase. *J. Immunol.* 163: 978–984.
9. Swantek, J. L., M. F. Tsen, M. H. Cobb, and J. A. Thomas. 2000. IL-1 receptor-associated kinase modulates host responsiveness to endotoxin. *J. Immunol.* 164: 4301–4306.
10. Wan, Y., H. Xiao, J. Affolter, T. W. Kim, K. Bulek, S. Chaudhuri, D. Carlson, T. Hamilton, B. Mazumder, G. R. Stark, et al. 2009. Interleukin-1 receptor-associated kinase 2 is critical for lipopolysaccharide-mediated post-transcriptional control. *J. Biol. Chem.* 284: 10367–10375.
11. Koziczak-Holbro, M., C. Joyce, A. Glück, B. Kinzel, M. Müller, C. Tschopp, J. C. Mathison, C. N. Davis, and H. Gram. 2007. IRAK-4 kinase activity is required for interleukin-1 (IL-1) receptor- and Toll-like receptor 7-mediated signaling and gene expression. *J. Biol. Chem.* 282: 13552–13560.
12. Kawagoe, T., S. Sato, A. Jung, M. Yamamoto, K. Matsui, H. Kato, S. Uematsu, O. Takeuchi, and S. Akira. 2007. Essential role of IRAK-4 protein and its kinase activity in Toll-like receptor–mediated immune responses but not in TCR signaling. *J. Exp. Med.* 204: 1013–1024.
13. Fraczek, J., T. W. Kim, H. Xiao, J. Yao, Q. Wen, Y. Li, J. L. Casanova, J. Pryjma, and X. Li. 2008. The kinase activity of IL-1 receptor-associated kinase 4 is required for interleukin-1 receptor/Toll-like receptor-induced TAK1-dependent NFκB activation. *J. Biol. Chem.* 283: 31697–31705.
14. Wu, Y. W., W. Tang, and J. P. Zuo. 2015. Toll-like receptors: potential targets for lupus treatment. *Acta Pharmacol. Sin.* 36: 1395–1407.
15. Bennett, L., A. K. Palucka, E. Arce, V. Cantrell, J. Borvak, J. Banchereau, and V. Pascual. 2003. Interferon and granulopoiesis signatures in systemic lupus erythematosus blood. *J. Exp. Med.* 197: 711–723.
16. Barrat, F. J., T. Meeker, J. Gregorio, J. H. Chan, S. Uematsu, S. Akira, B. Chang, O. Duramad, and R. L. Coffman. 2005. Nucleic acids of mammalian origin can act as endogenous ligands for Toll-like receptors and may promote systemic lupus erythematosus. *J. Exp. Med.* 202: 1131–1139.
17. Gilliet, M., W. Cao, and Y. J. Liu. 2008. Plasmacytoid dendritic cells: sensing nucleic acids in viral infection and autoimmune diseases. *Nat. Rev. Immunol.* 8: 594–606.
18. Avalos, A. M., L. Busconi, and A. Marshak-Rothstein. 2010. Regulation of autoreactive B cell responses to endogenous TLR ligands. *Autoimmunity* 43: 76–83.
19. Junt, T., and W. Barchet. 2015. Translating nucleic acid-sensing pathways into therapies. *Nat. Rev. Immunol.* 15: 529–544.
20. Christensen, S. R., J. Shupe, K. Nickerson, M. Kashgarian, R. A. Flavell, and M. J. Shlomchik. 2006. Toll-like receptor 7 and TLR9 dictate autoantibody specificity and have opposing inflammatory and regulatory roles in a murine model of lupus. *Immunity* 25: 417–428.
21. Torres-Salido, M. T., J. Cortés-Hernández, X. Vidal, A. Pedrosa, M. Vilardell-Tarrés, and J. Ordi-Ros. 2014. Neutrophil gelatinase-associated lipocalin as a biomarker for lupus nephritis. *Nephrol. Dial. Transplant.* 29: 1740–1749.
22. Guiducci, C., M. Gong, Z. Xu, M. Gill, D. Chaussabel, T. Meeker, J. H. Chan, T. Wright, M. Punaro, S. Bolland, et al. 2010. TLR recognition of self nucleic acids hampers glucocorticoid activity in lupus. *Nature* 465: 937–941.
23. Sun, J., N. Li, K. S. Oh, B. Dutta, S. J. Vayttaden, B. Lin, T. S. Ebert, D. De Nardo, J. Davis, R. Bagirzadeh, et al. 2016. Comprehensive RNAi-based screening of human and mouse TLR pathways identifies species-specific preferences in signaling protein use. *Sci. Signal.* 9: ra3.
24. Koziczak-Holbro, M., A. Glück, C. Tschopp, J. C. Mathison, and H. Gram. 2008. IRAK-4 kinase activity-dependent and -independent regulation of lipopolysaccharide-inducible genes. *Eur. J. Immunol.* 38: 788–796.
25. McElroy, W. T., Z. Tan, G. Ho, S. Paliwal, G. Li, W. M. Seganish, D. Tulshian, J. Tata, T. O. Fischmann, C. Sondey, et al. 2015. Potent and selective amidopyrazole inhibitors of IRAK4 that are efficacious in a rodent model of inflammation. *ACS Med. Chem. Lett.* 6: 677–682.
26. Kelly, P. N., D. L. Romero, Y. Yang, A. L. Shaffer, III, D. Chaudhary, S. Robinson, W. Miao, L. Rui, W. F. Westlin, R. Kapeller, and L. M. Staudt. 2015. Selective interleukin-1 receptor–associated kinase 4 inhibitors for the treatment of autoimmune disorders and lymphoid malignancy. *J. Exp. Med.* 212: 2189–2201.
27. Kondo, M., A. Tahara, K. Hayashi, M. Abe, H. Inami, T. Ishikawa, H. Ito, and Y. Tomura. 2014. Renoprotective effects of novel interleukin-1 receptor-associated kinase 4 inhibitor AS2444697 through anti-inflammatory action in 5/6 nephrectomized rats. *Naunyn Schmiedebergs Arch. Pharmacol.* 387: 909–919.
28. Yamamoto, M., S. Sato, H. Hemmi, K. Hoshino, T. Kaisho, H. Sanjo, O. Takeuchi, M. Sugiyama, M. Okabe, K. Takeda, and S. Akira. 2003. Role of adaptor TRIF in the MyD88-independent Toll-like receptor signaling pathway. *Science* 301: 640–643.
29. Kolanowski, S. T., M. C. Dieker, S. N. Lissenberg-Thunnissen, G. M. van Schijndel, S. M. van Ham, and A. ten Brinke. 2014. TLR4-mediated pro-inflammatory dendritic cell differentiation in humans requires the combined action of MyD88 and TRIF. *Innate Immun.* 20: 423–430.
30. Barrat, F. J., T. Meeker, J. H. Chan, C. Guiducci, and R. L. Coffman. 2007. Treatment of lupus-prone mice with a dual inhibitor of TLR7 and TLR9 leads to reduction of autoantibody production and amelioration of disease symptoms. *Eur. J. Immunol.* 37: 3582–3586.
31. Zhu, F. G., W. Jiang, L. Bhagat, D. Wang, D. Yu, J. X. Tang, E. R. Kandimalla, N. La Monica, and S. Agrawal. 2013. A novel antagonist of Toll-like receptors 7, 8 and 9 suppresses lupus disease-associated parameters in NZBW/F_1 mice. *Autoimmunity* 46: 419–428.
32. Teichmann, L. L., D. Schenten, R. Medzhitov, M. Kashgarian, and M. J. Shlomchik. 2013. Signals via the adaptor MyD88 in B cells and DCs make distinct and synergistic contributions to immune activation and tissue damage in lupus. *Immunity* 38: 528–540.
33. Gurkan, S., A. Cabinian, V. Lopez, M. Bhaumik, J. M. Chang, A. B. Rabson, and P. Mundel. 2013. Inhibition of type I interferon signalling prevents TLR ligand-mediated proteinuria. *J. Pathol.* 231: 248–256.
34. Motojima, M., T. Matsusaka, V. Kon, and I. Ichikawa. 2010. Fibrinogen that appears in Bowman's space of proteinuric kidneys in vivo activates podocyte Toll-like receptors 2 and 4 in vitro. *Nephron, Exp. Nephrol.* 114: e39–e47.
35. Tsai, P. Y., S. M. Ka, J. M. Chang, H. C. Chen, H. A. Shui, C. Y. Li, K. F. Hua, W. L. Chang, J. J. Huang, S. S. Yang, and A. Chen. 2011. Epigallocatechin-3-gallate prevents lupus nephritis development in mice via enhancing the Nrf2 antioxidant pathway and inhibiting NLRP3 inflammasome activation. *Free Radic. Biol. Med.* 51: 744–754.
36. Nanda, S. K., M. Lopez-Pelaez, J. S. C. Arthur, F. Marchesi, and P. Cohen. 2016. Suppression of IRAK1 or IRAK4 catalytic activity, but not type I IFN signaling, prevents lupus nephritis in mice expressing a ubiquitin binding–defective mutant of ABIN1. *J. Immunol.* 197: 4266–4273.
37. Furie, R., J. Merrill, V. Werth, M. Khamashta, K. Kalunian, P. Brohawn, G. Illei, J. Drappa, L. Wang, and S. Yoo. 2015. Anifrolumab, an anti-interferon-alpha receptor monoclonal antibody, in moderate to severe systemic lupus erythematosus (SLE). *Arthritis Rheumatol.* 67(Suppl. 10):3865–3868.
38. von Bernuth, H., C. Picard, A. Puel, and J. L. Casanova. 2012. Experimental and natural infections in MyD88- and IRAK-4-deficient mice and humans. *Eur. J. Immunol.* 42: 3126–3135.